



Motta, R. J. B., Almeida, A. Z. F., de Lima, B. L. B., Schneider, R., Balaban, R. D. C., van Duijneveldt, J. S., & de Oliveira, R. J. (2019). Polyphosphates can stabilize but also aggregate colloids. *Physical Chemistry Chemical Physics*, 2020(1), 15-19. [15].
<https://doi.org/10.1039/C9CP05225A>

Peer reviewed version

Link to published version (if available):
[10.1039/C9CP05225A](https://doi.org/10.1039/C9CP05225A)

[Link to publication record in Explore Bristol Research](#)
PDF-document

This is the author accepted manuscript (AAM). The final published version (version of record) is available online via Royal Society of Chemistry at <https://pubs.rsc.org/en/content/articlelanding/2019/cp/c9cp05225a#!divAbstract>. Please refer to any applicable terms of use of the publisher.

University of Bristol - Explore Bristol Research

General rights

This document is made available in accordance with publisher policies. Please cite only the published version using the reference above. Full terms of use are available:
<http://www.bristol.ac.uk/red/research-policy/pure/user-guides/ebr-terms/>

Cite this: DOI: 00.0000/xxxxxxxxxx

Polyphosphates can stabilize but also aggregate colloids[†]

Rayssa Jossanea Brasileiro Motta,^{a‡} Ana Zélia Falcão Almeida,^{a‡} Bruna Luiza Batista de Lima,^b Ricardo Schneider,^c Rosangela de Carvalho Balaban,^b Jeroen Sebastiaan van Duijneveldt^{*d} and Rodrigo José de Oliveira^{*a}

Received Date

Accepted Date

DOI: 00.0000/xxxxxxxxxx

Phosphates are well known as dispersants for a variety of colloidal particles. Here however we use rheological measurements to show that high molecular weight polyphosphates (PP) can instead act as a flocculant for Laponite clay platelets. The proposed mechanism is bridging of PP between clay particle edges, leading to highly charged clusters forming a Wigner glass. Dynamic light scattering shows a bimodal cluster size distribution, independent of PP molecular weight, but the highest molecular weight gave the highest viscous and loss moduli for the PP-clay solid. These unique all-inorganic solids may have application in solid-state ionic conducting materials, controlled release fertilizers and biomedical applications.

Phosphate anions find wide use as efficient deflocculants for colloidal systems^{1–4}. Rolfe, Miller and McQueen¹ studied characteristics of aqueous dispersions of the clay minerals montmorillonite, kaolin and illite using sodium tripolyphosphate ($\text{Na}_5\text{P}_3\text{O}_{10}$), sodium pyrophosphate ($\text{Na}_4\text{P}_2\text{O}_5$) and sodium hexametaphosphate ($(\text{NaPO}_3)_6$) as dispersing agents. They found that, depending on the length of the phosphate chains and sodium dissociation, the deflocculants varied in dispersion efficiency for

the various clay-water-phosphate systems. For example, sodium-saturated montmorillonite disperses very well in distilled water. A marginal improvement results from adding $\text{Na}_5\text{P}_3\text{O}_{10}$ or $(\text{NaPO}_3)_6$. Calcium-saturated montmorillonite however does not disperse into water. Adding the same phosphates to this system significantly improves the extent of dispersion. This is ascribed to interaction with exposed Al^{3+} sites on the clay particle edges, sequestration of Ca^{2+} ions and replacing these with Na^+ . As a further example, a ceramic paste with 70 wt% of kaolin can be made fluid through addition of sodium pyrophosphate at pH = 8⁵.

Phosphate anions are adsorbed quasi-irreversibly on the edges of clay particles (denoting the perimetral section around the clay discs perpendicular to the dominating surfaces) through ionic exchange, increasing the negative charge density of the particle edges and consequently electrostatic repulsion (note the particle faces are negatively charged already), giving rise to a more stable colloidal dispersion^{3,5}. Mongondry, Nicolai, and Tassin⁶ in their light scattering and rheology studies showed the influence of pyrophosphate on Laponite suspensions. Addition of 10 mM NaCl to a 2.5 wt% Laponite dispersion leads to rapid aggregation, whilst no aggregation is seen with 10 mM sodium pyrophosphate. The authors ascribe this to pyrophosphate adsorption at the positively charged edges inhibiting the formation of bonds between faces and edges. Ganley and van Duijneveldt³ found that the adsorption of pyrophosphate anions to montmorillonite platelet edges introduces negative charge to the particle surface, increasing the resistance of the elongated platelet clusters to contraction upon increase of ionic strength.

Whilst this colloidal stabilizing role of phosphates is well known for clay dispersions, there are also a few reports of percolation / aggregation induced by polyphosphates (PP). Tateyama et al.⁷ observed by X-ray diffractometry that tripolyphosphates - molecules consisting of three phosphate units - may induce a lamellar arrangement in aqueous clay dispersions, through ad-

^a Physical Chemistry of Materials Group, Departamento de Química, Universidade Estadual da Paraíba, Campina Grande, PB 58429-500, Brazil; E-mail: rodrigo@cct.uepb.edu.br

^b Laboratório de Pesquisa em Petróleo - LAPET, Universidade Federal do Rio Grande do Norte, Natal, RN 59078-970, Brazil.

^c Group of Polymers and Nanostructures, Universidade Tecnológica Federal do Paraná, Toledo, PR 85902-490, Brazil.

^d School of Chemistry, University of Bristol, Bristol BS8 1TS, UK. E-mail: J.S.VanDuijneveldt@bristol.ac.uk

[‡] Present address: Rayssa J. B. Motta: Instituto de Química e Biotecnologia, Universidade Federal de Alagoas; Ana Z. F. Almeida: Departamento de Química, Universidade Federal da Paraíba.

Electronic Supplementary Information (ESI) available: Sedimentation profile for sodium bentonite, calculations for Debye length, contour length and typical length scales. See DOI: 10.1039/x0xx00000x.

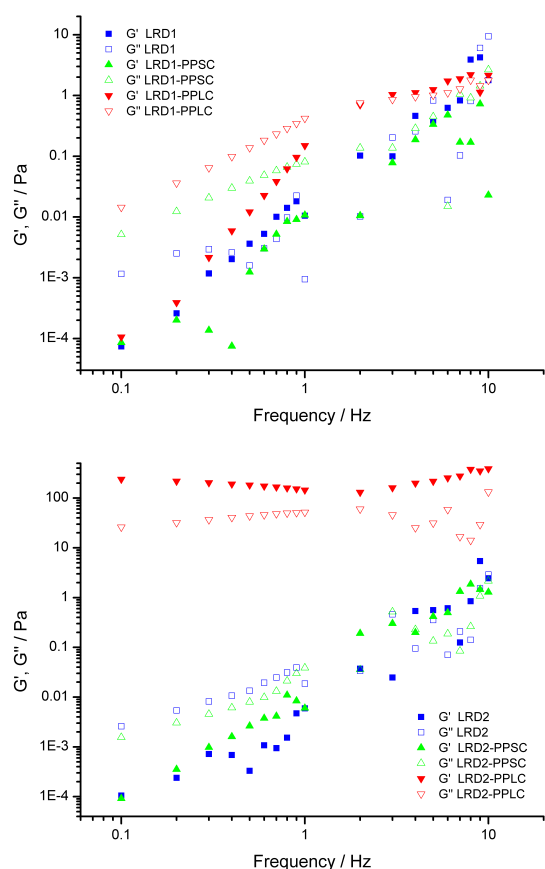


Fig. 1 Rheological characterization of LRD in water dispersions with and without PP (at $10^{-1} \text{ mol} \cdot \text{L}^{-1}$ of Na^+) for clay concentrations of 1 wt% (top) and 2 wt% (bottom). Measurements were made 36 h after dispersing the particles.

sorption across neighbouring edges, increasing the clay particle size. Penner and Lagaly⁸ stated that addition of (PP) to montmorillonite dispersions induced an increase in viscosity under certain conditions, and some kaolin pastes with PP may undergo gelation in a few hours when left undisturbed⁹. Yamaguchi et al.¹⁰ reported a reduced clay swelling upon addition of small amounts of DNA to dispersions of montmorillonite and beidellite.

PP are composed of orthophosphate monomers bound together as result of phosphate condensation¹¹, leading to chain lengths varying from a few units up to hundreds of phosphate units. Considering also that PP can make gels and arrested states in presence of Al^{3+} due to strong phosphate-aluminium bond formation^{12,13}, we propose that addition of PP can lead to arrested phases of clay particles by binding to multi-valent cations exposed at the particle edges. To test this hypothesis, we used aqueous dispersions of Laponite RD (LRD), from BYK. It is important to realize that LRD in water exfoliates into individual lamellae with a thickness of only 1 nm.¹⁴.

A simple experiment was done in order to evaluate if percolation can be obtained by PP bridging, preparing LRD dispersions in deionised water (1 and 2 wt%) with and without PPSC (short chain PP, with 20 orthophosphate units per chain, purchased from Sigma-Aldrich) and PPLC (long chain PP, with 100 orthophos-

phate units per chain, made according to Ref.¹⁵), both at $10^{-1} \text{ mol} \cdot \text{L}^{-1}$ of Na^+ counterions. LRD powder was dispersed directly into water or PP solutions, according to the desired sample. These dispersions resulted, over 36-48 h, in a viscous liquid, except for PPLC with LRD 2 wt% where an arrested phase was observed. Samples with sodium pyrophosphate, a well-known clay dispersing agent, were also made for comparison.

Rheological measurements were carried out using a Haake Mars rheometer from Thermo with a DC50 temperature controller, using a PP20Ti plate-plate geometry for the higher viscosity suspensions and a C60 / 2° Ti cone-plate geometry for the lower viscosity ones. Initially an amplitude scan was performed between 0.01 - 30 Pa, at a frequency of 1 Hz, with a pre-shear at a shear rate of 30 s^{-1} for 300 seconds. After a rest of 300 seconds, 31 points were collected with integration time of 10 seconds. The lowest stable stress in the linear viscoelastic region was selected, and a frequency sweep was measured from 10 to 0.1 Hz recording 9 points per decade with a minimum integration time of 10 s. All measurements were performed at room temperature (25°C).

The so-called "gel point" is taken as the oscillation frequency where elastic (G') and viscous (G'') modulus curves cross^{16,17}. It can be seen from Figure 1 that after 36 h the dispersion of LRD at 1 wt% in water (LRD1) has a frequency dependent viscoelasticity with no well-defined crossing of these two complex functions, in other words the sample is in the liquid state¹⁸. PP increases the elastic response of the arrested system, as can be seen in Figure 1 for the viscoelastic response of the material. There is an intense debate in the literature about how LRD particles self-assemble to make arrested states, and that is reflected in the fluidity of the dispersion, resembling a viscous liquid rather than a proper gel (See Figure 2). Following Ruzicka and Zaccarelli (2011)¹⁴, who reviewed the colloidal state of Laponite, one might anticipate that this viscous liquid would phase separate into a clay-rich phase and a clay-poor phase after a long time (months perhaps)¹⁹. The viscous liquid phase seen after 36 h for LRD1 is therefore in agreement with the current literature on phase diagrams for LRD where no arrested state is observed. For the LRD1-PPSC system, it is seen that again no clear gel point is observed, with the sample being a viscous fluid just like LRD1. Figure 1 shows that the viscous modulus of LRD1-PPSC is higher than that for LRD1, which may be the result from the known colloidal stabilizing role of PP chains after adsorbing at particle edges increasing negative surface charge density. When the chain size of PP is increased (LRD1-PPLC) keeping the phosphate concentration the same, the behaviour is opposite however and a gel point is clearly observed between 2-3 Hz. Images of these samples clearly demonstrate the difference in fluidity (Figure 2), resulting from the increase in attractive interactions promoted by PPLC. This is in contrast to the stabilizing behaviour commonly observed with low molecular weight phosphates.

Increasing the concentration of LRD particles to 2.0 wt% (LRD2) makes this change in behaviour more pronounced. One can see from Figure 2 that samples LRD2-PPSC and LRD2-PPLC are more viscous than LRD2, 36 h after preparation. That is clearly observed in rheological measurements presented in Figure 1. For LRD2 and LRD2-PPSC a gel point exists, but the frequency

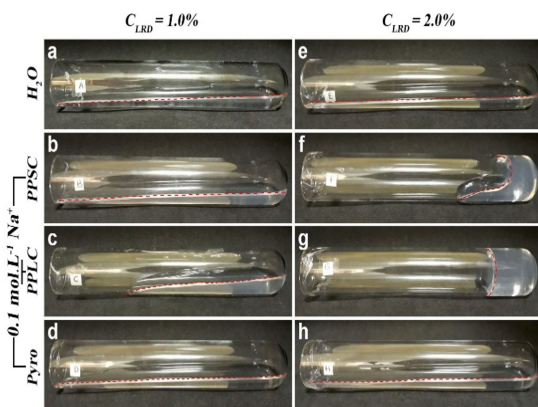


Fig. 2 Suspensions of LRD: (a) LRD1; (b) LRD1-PPSC; (c) LRD1-PPLC; (d) LRD suspension with sodium pyrophosphate ($C_{Na^+} = 10^{-1} \text{ mol} \cdot \text{L}^{-1}$); (e) LRD2; (f) LRD2-PPSC; (g) LRD2-PPLC; (h) LRD suspension with sodium pyrophosphate ($C_{Na^+} = 10^{-1} \text{ mol} \cdot \text{L}^{-1}$). Photos taken just after placing the test tubes on their side.

dependency of the viscous and elastic moduli suggests that these are only weakly arrested systems. The most dramatic result comes from the LRD2-PPLC system, which does not flow under gravity (Figure 2g).

The PP chains are highly charged, with a distance between charges of 0.26 nm^{20} - to be compared with the Bjerrum length of 0.72 nm , so charge condensation will occur. Moreover, the systems only contain Na^+ counterions (no added salt), giving a double layer thickness of 3.4 nm for 2 wt\% LRD (see ESI). Whilst the persistence length of these PP molecules has not been determined, it is likely that they adopt extended configurations, with a contour length of 2.4 nm for PPSC and 25.8 for PPLC (see ESI). It is instructive to compare these values with the typical separation between LRD particles of 40.5 nm at 2 wt\% (see ESI). The PPLC size is of similar order which explains why this long-chain PP is able to form particle bridges, whereas the PPSC is much shorter and is likely to only attach to one LRD particle at a time. We envisage that PP chains bind to clay edges in one or more locations along the chain - and in the case of PPLC, they may also act as bridges between two clay particles.

To amplify this point, further samples were made (Figure 2d and 2h) where LRD1 and LRD2 were made in sodium pyrophosphate (Pyro) at $0.1 \text{ mol} \cdot \text{L}^{-1} \text{ Na}^+$ concentration. Clay dispersions made in presence of Pyro fluidise easily, as demonstrated by Ganley and Duijneveldt³, and this is ascribed to Pyro molecules attaching to particle edges, increasing repulsions between clay particles. This behaviour is also seen for LRD samples with pyrophosphate⁶, demonstrating that the arrested phase observed for sample LRD2-PPLC is not merely due to an increase in ionic strength. This is illustrated in the ESI (Figure S2). Addition of 0.1 M of NaCl leads to aggregation. Aggregation and ultimately arrest also results when adding PPSC, but as this initially acts as a stabiliser, higher concentrations (0.5 M and above) are required to destabilise the particles (Figure S3).

To explore the role of particle shape, tests were also made using Sodium Bentonite (SB). An enhanced sedimentation rate shows that short-chain PP induces attractive interactions between SB

particles, however less so than addition of NaCl , showing that the PPSC here has a "traditional", stabilising role (see Electronic Supplementary Information for discussion and Figure S1). This may be ascribed to the role of edge contributions to the total surface area, which are very different for LRD and for SB, as can be seen from the platelet aspect ratio ($1:25$ for LRD but $1:300$ for SB)^{3,14}. As a result there is more scope for PPSC adsorption to enhance particle repulsions in the case of Laponite.

The rheology of LRD2-PPSC and LRD2-PPLC shows that the PP chain length is key to the formation of the observed arrested state. This is well known in the literature for various polymer-clay systems, but has not been reported previously for PP, as they are considered dispersants. For instance, Mongondry, Nicolai and Tassin⁶ demonstrated that pyrophosphate acts as dispersant - as does polyethylene oxide (PEO) at low molecular weights - however high molecular weight PEO is less effective which is ascribed to bridging occurring, similar to what we observe here when adding PP. A complex behaviour of clay suspensions was found upon addition of PEO^{21,22} and polyacrylate^{17,23}.

The clay - PPLC mixtures presented here are in an arrested state, but it is not possible yet to confirm if they are gels. Arrested systems can be made by either attractive or repulsive interactions, and an easy test for this was demonstrated by Ruzicka et al.²⁴. A gel formed by percolation due to attractive interactions will not solubilize easily in water, but a repulsive system (Wigner glass) solubilizes readily upon dilution. We submitted the LRD2-PPLC to this test.

Equal volumes of gel and water were mixed and left undisturbed in order to visually follow any solubilisation. It was found that, after 72 h , by putting the test tube horizontally the whole system fluidizes (not shown), demonstrating that the arrested phase was a Wigner glass. This repulsive arrested state is a result of particles or clusters that show steric or electrostatic mechanisms of surface stabilization. In order to propose a mechanism of formation for this arrested state, it is worth noting that samples LRD2-PPSC and LRD2-PPLC are more opaque and bluish than LRD2, which can be attributed to the presence of particle clusters large enough to scatter visible light. As LRD2 shows no opacity, it can be inferred that no aggregation is present, at least for the time span of our study. At this concentration of 2 wt\% LRD, Ruzicka and Zaccarelli described the formation of trapped states dominated by repulsive interactions¹⁴, the well-known Wigner glass state.

However, for the two samples containing PPSC and PPLC we conclude from the opacity that particle clusters are present. Figure 3 shows a dynamic light scattering characterization (Zetasizer Nano ZS90, Malvern) of such clusters obtained as a liquid dispersion after dilution of arrested samples, LRD2-PPSC and LRD2-PPLC, to a final clay concentration of 0.1 wt\% , with clusters in the size range $100\text{-}1000 \text{ nm}$ present in both cases. The majority of scattering objects (by volume) are around 32 nm and 91 nm (LRD2-PPSC) or 54 nm and 342 nm (LRD2-PPLC) reflecting single particles and small clusters. A lower volume contribution comes from large clusters with a diameter around $5 \mu\text{m}$ (but detecting such large clusters using DLS is difficult so care should be taken in making detailed interpretations). Ruzicka¹⁴ similarly re-

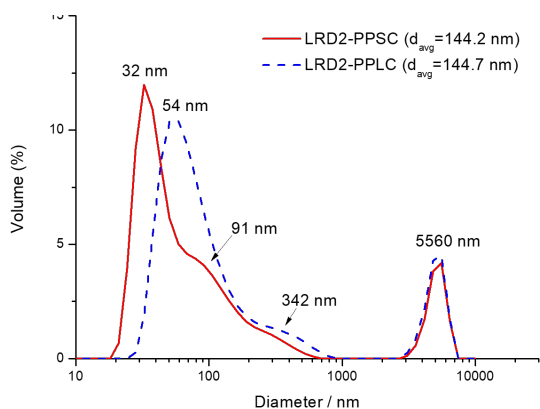


Fig. 3 Volume distribution from dynamic light scattering of LRD2-PPSC and LRD2-PPLC. Wigner glass dispersion samples after a 10× dilution.

ported LRD aggregates in equilibrium with individual platelets. We interpret the sample structure therefore as a Wigner glass made up of individual clay particles and clusters formed by PP bridged particles, with repulsive interactions. Furthermore, electrophoretic mobility measurements showed similar values for the LRD2-PPLC and LRD2-PPSC cluster dispersions ($-5.0 \pm 0.5 \times 10^{-8} \text{ m}^2/(\text{V}\cdot\text{s})$ and $-3.5 \pm 0.4 \times 10^{-8} \text{ m}^2/(\text{V}\cdot\text{s})$, respectively), and in both cases the mobility is negative as would be expected as both the clay faces and the PP chains are negatively charged. The slightly higher value for the PPLC sample may help to explain why this sample shows noticeably higher viscous and elastic moduli than the PPSC sample, as repulsions between clusters will be stronger. A detailed structural characterisation using X-ray scattering^{14,25} is left for future work.

This work opens up new ways for making functional materials based on easy bench chemistry with desired properties and functions. The resulting percolated clay-PP systems might be used as a true green controlled release fertilizer, as phosphorus could be leached to the soil via hydrolysis of the PP chains, leaving only natural clay as a by-product. Other potential applications include new gel-like media for plant growth, solid-state electrolytes, or matrices for luminescent molecules. Also, there are interesting perspectives of application as biomaterials, as it has been demonstrated that PP based particles can be active in bone and cartilage regeneration²⁶, microvascularization and angiogenesis^{27–29}, and PP chains can block cell cancer metastasis^{30,31}. Attractive interactions between clay particles and PP need to be further investigated, and it would be of interest to explore the role of branched-chains molecules, known as ultraphosphates³².

Phosphates adsorb to clay particle edges. In doing so they act as a dispersant for Laponite clay. For high molecular weight PP (100 phosphate units) however we find bridging between clay particles, resulting in a Wigner glass of repulsive Laponite-PP clusters.

Conflicts of interest

There are no conflicts to declare.

Acknowledgements

This work was funded by the Institute for Advanced Studies, through a Benjamin Meaker Visiting Professorship for RJdO, the Cabot Institute for the Environment of the University of Bristol, and CNPq (Universal Call). JvD and RJdO thank BYK for kindly donating Laponite RD. RJBM and AZFA thanks CAPES agency for a scholarship.

Notes and references

- B. Rolfe, R. Miller and I. McQueen, *Geol. Surv. Prof. Pap.*, 1987, 229.
- G. Lagaly, *Appl. Clay Sci.*, 1989, **4**, 105–123.
- W. J. Ganley and J. S. Van Duijneveldt, *Langmuir*, 2015, **31**, 4377–4385.
- A. Papo, L. Piani and R. Ricceri, *Colloids Surfaces A Physicochem. Eng. Asp.*, 2002, **201**, 219–230.
- G. Lagaly, *Coagulation, Second Ed.*, 2005, pp. 519–600.
- P. Mongondry, T. Nicolai and J. F. Tassin, *J. Colloid Interface Sci.*, 2004, **275**, 191–196.
- H. Tateyama, P. J. Scales, M. Ooi, S. Nishimura, K. Rees and T. W. Healy, *Langmuir*, 1997, **13**, 2440–2445.
- D. Penner and G. Lagaly, *Appl. Clay Sci.*, 2001, **19**, 131–142.
- W. B. Jepson, *Philos. Trans. R. Soc. London*, 1984, **311**, 411–432.
- N. Yamaguchi, S. Anraku, E. Paineau, C. R. Safinya, P. Davidson, L. J. Michot and N. Miyamoto, *Sci. Rep.*, 2018, **8**, year.
- F. Rashchi and J. A. Finch, *Miner. Eng.*, 2000, **13**, 1019–1035.
- E. C. de Oliveira Lima and F. Galembeck, *J. Colloid Interface Sci.*, 1994, **166**, 309–315.
- E. Skovroinski, R. J. de Oliveira and A. Galembeck, *Journal of Colloid and Interface Science*, 2018, **533**, 216–226.
- B. Ruzicka and E. Zaccarelli, *Soft Matter*, 2011, **7**, 1268–1286.
- A. Momeni and M. J. Filiaggi, *J. Non. Cryst. Solids*, 2013, **382**, 11–17.
- J. Labanda and J. Llorens, *J. Colloid Interface Sci.*, 2005, **289**, 86–93.
- J. Labanda, J. Sabaté and J. Llorens, *Colloids Surfaces A Physicochem. Eng. Asp.*, 2007, **301**, 8–15.
- H. A. Barnes, *A handbook of elementary rheology*, University of Wales, Institute of Non-Newtonian Fluid Mechanics, Aberystwyth, 2000, vol. 331, pp. 868–869.
- R. Angelini, B. Ruzicka, E. Zaccarelli, L. Zulian, M. Sztucki, A. Moussaïd, T. Narayanan and F. Sciortino, *AIP Conf. Proc.*, 2013, **1518**, 384–390.
- P. Mongondry, J. F. Tassin and T. Nicolai, *J. Colloid Interface Sci.*, 2005, **283**, 397–405.
- L. Zulian, F. Augusto De Melo Marques, E. Emilietri, G. Ruocco and B. Ruzicka, *Soft Matter*, 2014, **10**, 4513–4521.
- B. Zheng and S. R. Bhatia, *Colloids Surfaces A Physicochem. Eng. Asp.*, 2017, **520**, 729–735.
- J. Labanda and J. Llorens, *Colloids Surfaces A Physicochem. Eng. Asp.*, 2004, **249**, 127–129.
- B. Ruzicka, L. Zulian, E. Zaccarelli, R. Angelini, M. Sztucki, A. Moussaïd and G. Ruocco, *Phys. Rev. Lett.*, 2010, **104**, 1–4.
- A. Shalkevich, A. Stradner, S. K. Bhat, F. Mulle and P. Schurtenberger, *Langmuir*, 2007, **23**, 3570–3580.
- X. Wang, H. C. Schröder and W. E. Müller, *J. Mater. Chem. B*, 2018, **6**, 2385–2412.
- S. A. Smith, N. J. Mutch, D. Baskar, P. Rohloff, R. Docampo and J. H. Morrissey, *Proc. Natl. Acad. Sci. U. S. A.*, 2006, **103**, 903–908.
- J. H. Yeon, N. Mazinani, T. S. Schlappi, K. Y. Chan, J. R. Baylis, S. A. Smith, A. J. Donovan, D. Kudela, G. D. Stucky, Y. Liu, J. H. Morrissey and C. J. Kastrup, *Sci. Rep.*, 2017, **7**, 1–10.
- Z. Gu, H. Xie, L. Li, X. Zhang, F. Liu and X. Yu, *J. Mater. Sci. Mater. Med.*, 2013, **24**, 1251–1260.
- K. Y. Han, B. S. Hong, Y. J. Yoon, C. M. Yoon, Y. K. Kim, Y. G. Kwon and Y. S. Gho, *Biochem. J.*, 2007, **406**, 49–55.
- E. V. Kulakovskaya, M. Y. Zemskova and T. V. Kulakovskaya, *Biochem.*, 2018, **83**, 961–968.
- G. Palavit, C. Mercier, L. Montagne, M. Drache and Y. Abe, *J. Am. Ceram. Soc.*, 2005, **81**, 1521–1524.